

Catalytic conversion of methane and CO₂ to synthesis gas over a La₂O₃-modified SiO₂ supported Ni catalyst in fluidized-bed reactor

Jing Gao^a, Zhaoyin Hou^{a,*}, Jianzhong Guo^{a,b},
Yinghong Zhu^c, Xiaoming Zheng^{a,*}

^a Institute of Catalysis, Department of Chemistry, Zhejiang University (Xixi Campus), Hangzhou 310028, China

^b Department of Chemistry, Zhejiang Forestry University, 311300 Lin'an, China

^c College of Chemical Engineering and Materials, Zhejiang University of Technology, Hangzhou 310012, China

Available online 26 November 2007

Abstract

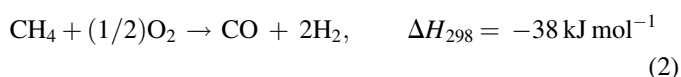
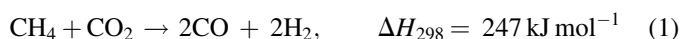
In this contribution, a commercial spherical SiO₂ was modified with different amounts of La₂O₃, and used as the support of Ni catalysts for autothermal reforming of methane in a fluidized-bed reactor. Nitrogen adsorption, XRD and H₂-TPR analysis indicated that La₂O₃-modified SiO₂ had higher surface area, strengthened interaction between Ni and support, and improved dispersion of Ni. CO₂-TPD found that La₂O₃ increased the alkalinescence of SiO₂ and improved the activation of CO₂. Coking reaction (via both temperature-programmed surface reaction of CH₄ (CH₄-TPSR) and pulse decomposition of CH₄) disclosed that La₂O₃ reduced the dehydrogenation ability of Ni. CO₂-TPO, O₂-TPO (followed after CH₄-TPSR) confirmed that only part amount of carbon species derived from methane decomposition could be removed by CO₂, and O₂ in feed played a crucial role for the gasification of the inactive surface carbons. Ni/*x*La₂O₃-SiO₂ (*x* = 10, 15, 30) possessed high activity and excellent stability for autothermal reforming of methane in a fluidized-bed reactor.

© 2007 Elsevier B.V. All rights reserved.

Keywords: Autothermal reforming of methane; Ni/La₂O₃-SiO₂ catalysts; Synthesis gas; Fluidized-bed reactor

1. Introduction

Methane autothermal reforming with CO₂ and oxygen (abbreviated as MATR) has been a substantial interest in recent years in attractive alternative routes for conversion of natural gas (methane) to synthesis gas for its low-energy requirement and a wide range of H₂/CO ratio by manipulating the relative concentrations of CO₂ and O₂ in feed [1–10]. At the same time, Ruckenstein and Hu recommended that this combined reactions could overcome the explosions that can occur during the partial oxidation of methane [11].



In published papers, the MATR process is carried out mainly in a fixed bed reactor, in which the combined reactions take place in two separate reaction zones—a part of methane is combusted into CO₂ and steam to ensure the complete conversion of the oxygen in feed in the inlet zone, and the unconverted methane is reformed to synthesis gas by CO₂ and steam in the second zone. A significant temperature gradient in the catalyst bed formed, which ultimately resulted in the thermal sintering and deactivation of catalyst [12–14]. In order to overcome this limitation of the MATR process in fixed bed reactor, a lot of noble metals (Ir, Pt and Rh) [1,6,7], noble metal-promoted Ni (Pt–Ni) [10,15] and alkaline-earth metal oxides supported Ni, Co catalysts [5,8,11,16] were reported.

Ashcroft reported that 1% Ir/Al₂O₃ catalyst possessed high yields of synthesis gas at 1050 K, without carbon deposition [1]. O'Connor found that the Pt/ZrO₂ was least prone to deactivation among a series of supported transition metals [6]. Souza and co-workers compared Pt/Al₂O₃, Pt/ZrO₂, and Pt/10%ZrO₂/Al₂O₃ catalysts, and they found that Pt/10%ZrO₂/Al₂O₃ was the most active and stable catalyst for this process [7]. Ruckenstein and Hu found that about 90% conversion of

* Corresponding authors. Tel.: +86 571 88273272; fax: +86 571 88273283.
E-mail address: zyhou@zju.edu.cn (Z. Hou).

CH₄ and about 98% selectivity to CO and H₂ were obtained at 790 °C over NiO/MgO solid solution, while the reduced NiO/SiO₂ and NiO/Al₂O₃ catalysts provided lower activities and stabilities compared to the reduced NiO/MgO [11]. Choudhary [8] found that coke formation was a serious problem for CO₂ reforming over NiO/CaO catalyst but little or no coke was found in the MATR. Ruckenstein and Hu also reported that Co/MgO catalysts had high activity and selectivity in the combined reactions [5].

Tomishige [9,10,15,17] and Zheng [3,18] suggested that the high rates of heat transfer and high stability of operation could be obtained in a fluidized-bed reactor owing to the enhanced abilities in heat transfer and fluidization of catalyst. But the selected catalyst must be well shaped and possess excellent wearability because the attrition of catalyst particles is a serious problem in the fluidized-bed reactor.

Ni/La₂O₃ catalyst in dry reforming of methane was thoroughly investigated by Verykios's group. It was found that CO₂ favorably adsorbed on the La₂O₃ support and induced the formation of surface carbonate species, which accelerated the gasification of surface carbon species from methane dehydrogenation [19–23]. But abundant experience is necessary in order to prepare a successful Ni/La₂O₃ catalyst, as neither Hou [24] nor Lu [25] can repeat these results in their papers. At the same time, it is quite difficult to use pure La₂O₃-supported Ni catalyst in a fluidized-bed reactor for its lower mechanical strength and higher price.

In this contribution, one kind of spherical SiO₂ particle with higher abrasive hardness and lower price was modified by La₂O₃ and used as the support of Ni catalysts for autothermal reforming in a fluidized-bed reactor. The physicochemical properties of the La₂O₃-modified SiO₂ and its supported Ni catalysts were characterized by nitrogen adsorption, X-ray diffraction (XRD) and temperature-programmed reduction (H₂-TPR). Methane activation on Ni/La₂O₃-SiO₂ catalysts at different atmosphere (CH₄, CH₄/CO₂ and CH₄/O₂) and CO₂ activation on La₂O₃-modified SiO₂ were investigated. And the reactivity of surface carbons (derived from CH₄ dehydrogenation) with CO₂ and O₂ was further characterized.

2. Experimental

2.1. Catalysts preparation

A series of La₂O₃-modified SiO₂ denoted as *x*La₂O₃-SiO₂ (*x* = 5, 10, 15, 30), where *x* means the amount of La₂O₃ (wt%) added in SiO₂, were prepared by impregnation of a commercial spherical SiO₂ into an aqueous solution of lanthanum nitrate. The precursor supports were dried at 110 °C overnight, and calcined at 700 °C for 4 h. And then, these modified supports were impregnated into an aqueous solution of Ni(NO₃)₂ with a controlled Ni loading amount (5 wt% of the support). The precursors were dried at 80 °C in vacuum and calcined at 800 °C in stagnant air for 4 h.

2.2. The physicochemical properties of *x*La₂O₃-SiO₂ and Ni/*x*La₂O₃-SiO₂

The physicochemical properties of the La₂O₃-modified SiO₂ and *x*La₂O₃-SiO₂ supported Ni catalysts were characterized by nitrogen adsorption, XRD and H₂-TPR.

The structures of the modified supports were measured by nitrogen adsorption at −196 °C using an OMNISORP 100CX system (Coulter Co., USA). All samples were pretreated at 250 °C for 2 h in high vacuum. Pore size distribution, pore volume and its surface area were calculated on the isotherm of adsorption by a Barrett–Joyner–Halenda method [26].

XRD spectra of *x*La₂O₃-SiO₂ supported Ni catalysts were obtained with a PW 3040/60 diffractometer (Philips, Holland) using nickel-filtered Cu Kα radiation at 40 kV and 40 mA. Diffraction data were recorded using continuous scanning with a rate of 0.04 °/s.

H₂-TPR of the *x*La₂O₃-SiO₂ supported Ni catalysts was carried out in a quartz reactor equipped with an on-line mass spectrometer (OmniStar™, GSD301, Switzerland). Samples (100 mg) were first treated at 750 °C in Ar for 1 h, cooled to 100 °C. Then shifted to 10% H₂-Ar and heated linearly at 20 °C/min to 850 °C. H₂ (*m/e* = 2) and produced H₂O (*m/e* = 18) in effluent were detected and recorded continuously as functions of temperature.

2.3. CO₂ activation on La₂O₃-SiO₂

CO₂ activation on La₂O₃-SiO₂ was investigated via CO₂-TPD. In this experiment, all samples were first treated in Ar at 750 °C for 1 h, cooled to 50 °C. And then exposed to 20% CO₂ (50 ml/min, Ar in balance) for 30 min, purged in Ar for 1 h at 100 °C and heated linearly at 15 °C/min to 750 °C in 50 ml/min Ar. CO₂ (*m/e* = 44) in effluent was recorded continuously as functions of temperature.

2.4. Methane activation and catalytic conversion on Ni/*x*La₂O₃-SiO₂

Methane activation and catalytic conversion on Ni/*x*La₂O₃-SiO₂ catalysts at different atmosphere (CH₄, CH₄/CO₂ and CH₄/O₂) were investigated via pulse experiment. Pulse experiments were carried out in the same equipment as H₂-TPR. The catalysts were first reduced under H₂ flow at 700 °C for 1 h. CH₄, CH₄/O₂ (2:1) or CH₄/CO₂ (1:1) pulse was introduced with a 6-port gas-sampling valve (total volume 500 μl with 250 μl CH₄ and Ar in balance). The reaction temperature was maintained at 700 °C. All gases in effluent were recorded as a function of temperature, the turnover frequency of methane (TOF, defined as (mole of CH₄ converted)/(mole of Ni atom) per second) was calculated on the basis of methane conversion.

2.5. The reactivity of surface carbons on Ni/La₂O₃-SiO₂

The reactivity of surface carbons (derived from CH₄ dehydrogenation) with CO₂ and O₂ was investigated via

coking reaction (CH_4 -TPSR) and consecutively followed CO_2 -TPO, O_2 -TPO. Before these experiments, catalysts were reduced under H_2 flow at 700°C for 1 h, cooled to 50°C in Ar. And then shifted to 10% CH_4/Ar (50 ml/min), heated to 800°C at a ramp of $15^\circ\text{C}/\text{min}$ and hold at 800°C for 20 min. After coking reaction, CO_2 -TPO was performed in 10% CO_2/Ar from 50°C to 800°C at a ramp of $15^\circ\text{C}/\text{min}$. Followed O_2 -TPO was carried out in a flow of 10% O_2/Ar from 50°C to 800°C at $15^\circ\text{C}/\text{min}$. All gases in effluent were recorded as functions of temperature by a quadrupole mass spectrometer (OmniStarTM, GSD301, Switzerland). At the same time, the amount of carbons formed after coking reaction and residual carbons after CO_2 -TPO were detected via TG (PE-TGA7, USA) from 50°C to 900°C .

2.6. MATR on $\text{Ni}/\text{La}_2\text{O}_3\text{-SiO}_2$

MATR was carried out in a fluidized-bed quartz reactor (i.d. = 12 mm) at atmospheric pressure. CH_4 (99.99%), CO_2 (99.9%) and O_2 (99.9%) were introduced into the reactor controlled by three sets of mass flow controller (Brooks, 5850E, USA) at a molar ratio of $\text{CH}_4:\text{CO}_2:\text{O}_2 = 10:4:3$ and the total flow rate was controlled at 300 ml/min. Catalyst (2 ml, about 1.0 g) was first pretreated in H_2 at 700°C for 1 h at atmospheric pressure. The effluent gas was cooled in an ice-water trap and analyzed with an on-line gas chromatograph (Shimadzu, GC-8A) equipped with a packed column (TDX-01) and a thermal conductivity detector.

3. Results and discussion

3.1. The physicochemical properties of the $x\text{La}_2\text{O}_3\text{-SiO}_2$ and $\text{Ni}/x\text{La}_2\text{O}_3\text{-SiO}_2$

The surface areas and the pore structure of different amount of La_2O_3 -modified SiO_2 supports are summarized in Table 1. The surface area and the cumulative pore volume decreased continuously with the increasing La_2O_3 content due to deposition of La_2O_3 on the surface of SiO_2 . The surface area decreased from $330.0\text{ m}^2/\text{g}$ (of pure SiO_2) to $193.3\text{ m}^2/\text{g}$ (of $30\text{La}_2\text{O}_3\text{-SiO}_2$). But it was interesting to find that the detected surface area of La_2O_3 -modified SiO_2 is several times higher than that of pure La_2O_3 ($<30\text{ m}^2/\text{g}$) [24,25].

Fig. 1 is the XRD spectra of the fresh La_2O_3 -modified SiO_2 supported Ni catalysts. Only in Ni/SiO_2 and $\text{Ni}/5\text{La}_2\text{O}_3\text{-SiO}_2$, the crystalline phase of nickel oxide was detected. But the

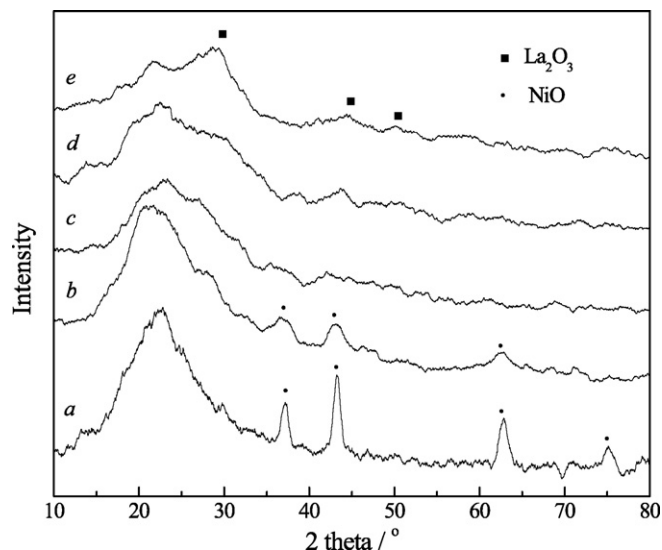


Fig. 1. XRD spectra of different catalysts. (a) NiO/SiO_2 , (b) $\text{NiO}/5\text{La}_2\text{O}_3\text{-SiO}_2$, (c) $\text{NiO}/10\text{La}_2\text{O}_3\text{-SiO}_2$, (d) $\text{NiO}/15\text{La}_2\text{O}_3\text{-SiO}_2$ and (e) $5\text{NiO}/30\text{La}_2\text{O}_3\text{-SiO}_2$.

diffraction peaks become broader in $\text{Ni}/5\text{La}_2\text{O}_3\text{-SiO}_2$. According to Scherrer–Warren equation, the calculated NiO particles sizes in Ni/SiO_2 and $\text{Ni}/5\text{La}_2\text{O}_3\text{-SiO}_2$ on the basis of half width of NiO (200) were 10.9 nm and 4.9 nm, respectively. When the amount of La_2O_3 in modified supports are more than 10 wt%, no NiO diffraction peaks could be detected, which inferred that NiO was highly dispersed on the modified SiO_2 .

The XRD spectra of the reduced catalysts are shown in Fig. 2. Sharp diffraction peaks of Ni were detected in pure SiO_2 supported Ni catalysts, and the calculated Ni particle sizes according to Scherrer–Warren equation on the basis of half width of Ni (111) was 45.0 nm. The diffraction peaks of Ni are broader and weaker on the surface of La_2O_3 -modified SiO_2 supports, and the calculated Ni particles sizes rapidly decreased to less than 6.0 nm with the added La_2O_3 . And this particle size is smaller than that of pure La_2O_3 -supported Ni catalysts [22],

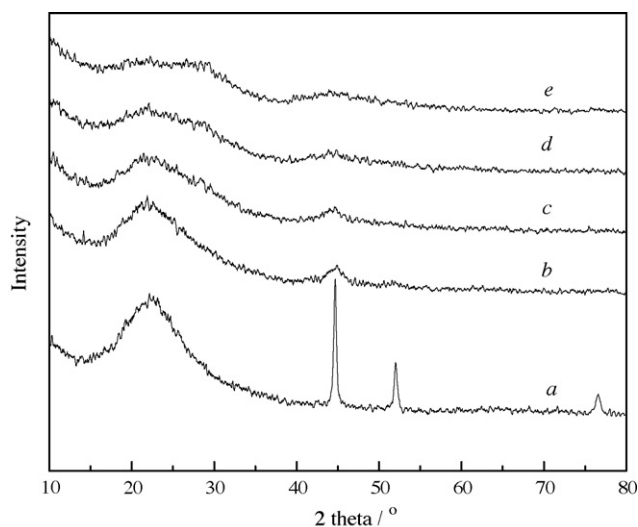


Fig. 2. XRD spectra of the reduced catalysts. (a) Ni/SiO_2 , (b) $\text{Ni}/5\text{La}_2\text{O}_3\text{-SiO}_2$, (c) $\text{Ni}/10\text{La}_2\text{O}_3\text{-SiO}_2$, (d) $\text{Ni}/15\text{La}_2\text{O}_3\text{-SiO}_2$ and (e) $\text{Ni}/30\text{La}_2\text{O}_3\text{-SiO}_2$.

Table 1
The structure of La_2O_3 -modified SiO_2

Supports	S_{BET} (m^2/g)	Pore structure		
		D_p (nm)	V_p (cm^3/g)	S_p (m^2/g)
SiO_2	330.0	18.0	1.13	328.0
$5\text{La}_2\text{O}_3\text{-SiO}_2$	288.6	18.2	0.98	281.2
$10\text{La}_2\text{O}_3\text{-SiO}_2$	259.7	18.4	0.92	259.9
$15\text{La}_2\text{O}_3\text{-SiO}_2$	252.4	18.7	0.89	257.1
$30\text{La}_2\text{O}_3\text{-SiO}_2$	193.3	20.9	0.72	201.8

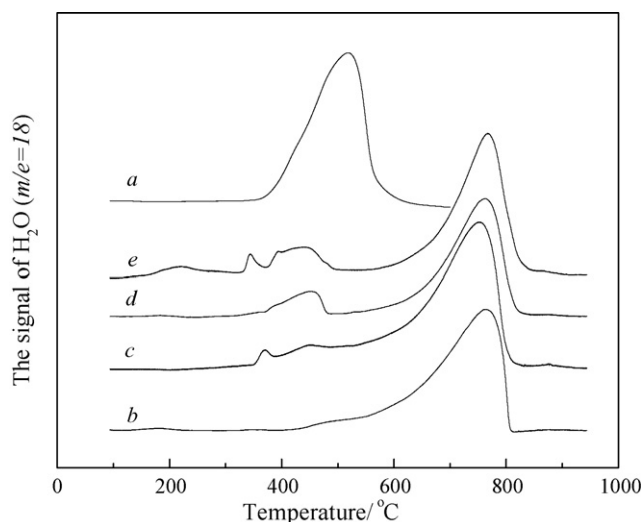


Fig. 3. The H_2 -TPR profile of the different catalysts. (a) NiO/SiO_2 , (b) $\text{NiO}/5\text{La}_2\text{O}_3\text{-SiO}_2$, (c) $\text{NiO}/10\text{La}_2\text{O}_3\text{-SiO}_2$, (d) $\text{NiO}/15\text{La}_2\text{O}_3\text{-SiO}_2$ and (e) $\text{NiO}/30\text{La}_2\text{O}_3\text{-SiO}_2$.

which might be contributed to the higher surface area of La_2O_3 -modified SiO_2 than that of pure La_2O_3 . These results confirmed that La_2O_3 in SiO_2 improved the dispersion of Ni partly due to formation of La_2NiO_4 [16].

The TPR profiles of La_2O_3 -modified SiO_2 supported Ni catalysts are depicted in Fig. 3. On pure SiO_2 , there is only one reduction peak at about 520°C , assigned to the reduction of “free state” NiO with weak interaction with support [18,27,28]. This kind of NiO existed in big particles (10.9 nm in this contribution) and could be reduced easily. Ni phase formed from this kind of NiO easily migrate and aggregate during the reduction and reaction process [29]. In this research, the detected Ni particles size on pure SiO_2 support aggregated to 45.0 nm only after reduction in H_2 .

The maximum reduction temperature of NiO increased obviously to about 770°C on the surface of La_2O_3 -modified SiO_2 . This kind of NiO species existed in smaller particles (less than 6.0 nm in this paper), is assigned to the “bound state” due to strong interaction between Ni and the modified SiO_2 . Ni particles reduced from this “bound state” NiO had strong support–metal interaction, which hindered the migration and aggregation of reduced Ni particle, and Ni particles remained in higher dispersion. This increased reduction temperature of NiO might be contributed to the formation of La_2NiO_4 , which must be reduced above 600°C [16]. The low temperature peaks (380°C and 420°C) in $\text{Ni}/x\text{La}_2\text{O}_3\text{-SiO}_2$ ($x = 10, 15, 30$) are assigned to the reduction of the “free state” NiO and the amount of this kind of NiO increased slightly with the added amount of La_2O_3 in support. But no agglomeration of Ni particle in the reduced La_2O_3 -modified SiO_2 support was detected (see the XRD spectrum in Fig. 2). These results indicate that La_2O_3 could be unevenly distributed within the silica spheres, and La_2O_3 could make Ni particle insulated and retard its agglomeration [30].

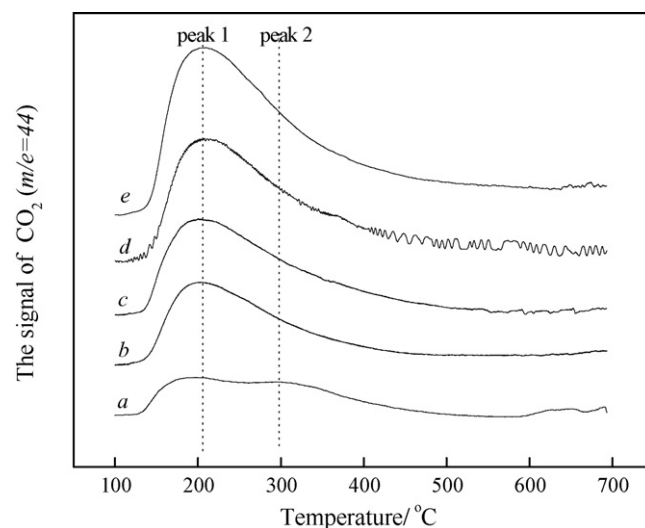


Fig. 4. CO_2 -TPD profiles of different supports. (a) SiO_2 , (b) $5\text{La}_2\text{O}_3\text{-SiO}_2$, (c) $10\text{La}_2\text{O}_3\text{-SiO}_2$, (d) $15\text{La}_2\text{O}_3\text{-SiO}_2$ and (e) $30\text{La}_2\text{O}_3\text{-SiO}_2$.

3.2. CO_2 activation on $x\text{La}_2\text{O}_3\text{-SiO}_2$

CO_2 -TPD profiles of La_2O_3 -modified SiO_2 are shown in Fig. 4. Two carbon dioxide desorption peaks were observed at 210°C and 300°C . And the total amount of desorbed CO_2 increased obviously with the increasing La_2O_3 content. These results indicate that La_2O_3 favors the adsorption and activation of CO_2 . This enhanced activity was thoroughly investigated by Verykios's groups, which was contributed to the formation of $\text{La}_2\text{O}_2\text{CO}_3$ and formate species [19–22] and these species could accelerate the elimination of the surface carbonaceous species such as CH_x ($x = 0\text{--}3$) during the reforming process.

3.3. Methane activation and catalytic conversion over $\text{Ni}/x\text{La}_2\text{O}_3\text{-SiO}_2$

Methane activation and catalytic conversion over $\text{Ni}/\text{La}_2\text{O}_3\text{-SiO}_2$ catalysts in different atmosphere (CH_4 , $\text{CH}_4\text{-O}_2$ and $\text{CH}_4\text{-CO}_2$) were investigated via pulse experiment. The calculated turnover frequency of methane (TOF) on Ni/SiO_2 and $\text{Ni}/30\text{La}_2\text{O}_3\text{-SiO}_2$ are summarized in Table 2.

For methane decomposition (only pure CH_4 was pulsed), Ni/SiO_2 exhibited a higher initial activity (the calculated TOF was 9.8 s^{-1}), and decreased with the increasing pulse number due to the carbon deposition on the surface of Ni. The calculated TOF of CH_4 on $\text{Ni}/30\text{La}_2\text{O}_3\text{-SiO}_2$ decreased to 7.7 s^{-1} . These data are comparable with that summarized in reference [31], which disclosed that La_2O_3 reduced the dehydrogenation ability of Ni catalyst. With the appearance of CO_2 and O_2 in feed, the detected TOF of CH_4 was enhanced a lot compared with the single CH_4 decomposition. In $\text{CH}_4\text{-CO}_2$ atmosphere, the TOF of CH_4 reached 20.6 s^{-1} on $\text{Ni}/30\text{La}_2\text{O}_3\text{-SiO}_2$, and 16.4 s^{-1} on Ni/SiO_2 . In $\text{CH}_4\text{-O}_2$ atmosphere, these data increased to 15.6 s^{-1} and 15.8 s^{-1} , respectively. These results indicated that both CO_2 and O_2 accelerated the conversion of methane, but CO_2 was more effective on $\text{Ni}/30\text{La}_2\text{O}_3\text{-SiO}_2$, which could be

Table 2

Methane turnover frequency (TOF) in different atmosphere (CH_4 , CH_4/CO_2 and CH_4/O_2) over Ni/SiO_2 and $\text{Ni}/30\text{La}_2\text{O}_3\text{-SiO}_2$

Pulse number	CH_4 decomposition (TOF (s^{-1}))		CH_4/O_2 (TOF (s^{-1}))		CH_4/CO_2 (TOF (s^{-1}))	
	Ni/SiO_2	$\text{Ni}/30\text{La}_2\text{O}_3\text{-SiO}_2$	Ni/SiO_2	$\text{Ni}/30\text{La}_2\text{O}_3\text{-SiO}_2$	Ni/SiO_2	$\text{Ni}/30\text{La}_2\text{O}_3\text{-SiO}_2$
1	9.8	7.7	15.6	15.8	16.4	20.6
2	7.6	7.0	15.2	15.6	15.8	18.0
3	7.0	6.7	12.1	14.9	15.4	17.6
4	6.8	6.7	11.3	12.8	15.4	15.9
5	6.3	6.6	11.4	10.3	12.0	14.8

demonstrated from the increased adsorption and activation of CO_2 by La_2O_3 in the form of $\text{La}_2\text{O}_3\text{CO}_3$, which in turn accelerated the conversion of methane [19–22].

3.4. The reactivity of surface carbons on $\text{Ni}/x\text{La}_2\text{O}_3\text{-SiO}_2$

3.4.1. Coking reaction

Fig. 5(A) and (B) shows the MS signals of effluent gases during the coke reaction step via CH_4 -TPSR on Ni/SiO_2 and $\text{Ni}/30\text{La}_2\text{O}_3\text{-SiO}_2$, respectively. Three CH_4 decomposition peaks were detected within the temperature range of 410–800 °C on Ni/SiO_2 , while four peaks were detected in the range

of 380–700 °C on $\text{Ni}/30\text{La}_2\text{O}_3\text{-SiO}_2$. These peaks could be assigned to different kind CH_x species formed according to reference [32].

The significant difference on Ni/SiO_2 and $\text{Ni}/30\text{La}_2\text{O}_3\text{-SiO}_2$ is the amount of carbon species formed via CH_4 decomposition, which are 12.9 mmol/g-cat and 1.9 mmol/g-cat (calculated via TG analysis), respectively (Table 3). According to the recommended coke formation mechanism [33–38], the heavy coke deposition on Ni/SiO_2 was contributed to that encapsulating carbon and whisker carbon formed easily on the surface of bigger sized Ni particles.

3.4.2. The reactivity of surface carbons with CO_2 and O_2

The reactivity of the carbon species deposited on La_2O_3 -modified SiO_2 supported Ni catalysts from CH_4 decomposition were investigated via CO_2 -TPO and consecutively followed by O_2 -TPO shown in Fig. 6. In CO_2 -TPO, 10.4 mmol-coke/g-cat formed on Ni/SiO_2 catalyst during coke reaction was removed by CO_2 (Table 3). On the surface of the La_2O_3 -modified SiO_2 supported Ni catalysts, the detected CO in effluent decreased continuously with the increasing amount of La_2O_3 . On $\text{Ni}/30\text{La}_2\text{O}_3\text{-SiO}_2$, only 1.9 mmol-coke/g-cat formed during coke reaction and 1.4 mmol-coke/g-cat was removed by CO_2 (Table 3).

It was found that some amount of carbon still remained after CO_2 -TPO (even at 800 °C). In the effluent of O_2 -TPO, CO_2 (formed via the reaction between the remained carbons with O_2) was detected, which suggested that this part of surface carbons was inactive in CO_2 atmosphere. According to published data, this kind of inactive surface carbon are mainly graphite [39,40], would accumulate and bring a heavy carbon deposition, which is a main drawback of the dry reforming process [2,7,39–42]. The amount of detected inactive surface carbon decreased from 2.5 mmol-coke/g-cat (over Ni/SiO_2) to 0.5 mmol-coke/g-cat (over $\text{Ni}/30\text{La}_2\text{O}_3\text{-SiO}_2$) (Table 3). In this aspect, O_2 in feed in the autothermal reforming process is very important in solving coke deposition in CH_4 reforming.

3.5. Autothermal reforming of methane over $\text{Ni}/x\text{La}_2\text{O}_3\text{-SiO}_2$

The time-dependent conversions of CH_4 on $\text{Ni}/x\text{La}_2\text{O}_3\text{-SiO}_2$ catalysts in the fluidized-bed reactor are plotted in Fig. 7. It can be found that pure SiO_2 supported Ni catalyst was rapidly deactivated during 5 h on stream, while $\text{Ni}/5\text{La}_2\text{O}_3\text{-SiO}_2$ only

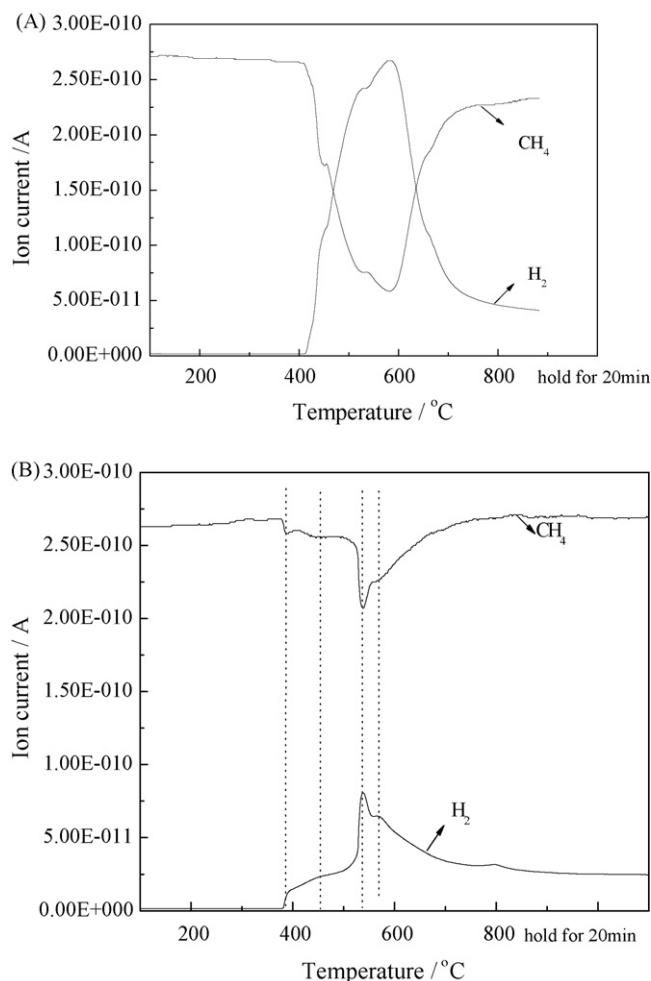


Fig. 5. MS signal in CH_4 -TPSR (A) Ni/SiO_2 and (B) $\text{Ni}/30\text{La}_2\text{O}_3\text{-SiO}_2$.

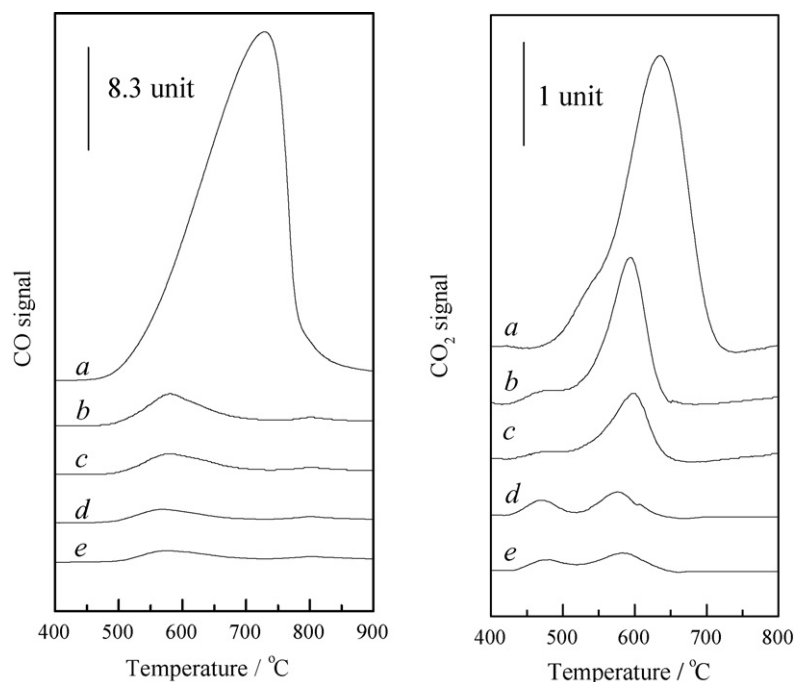


Fig. 6. CO₂-TPO (left) and O₂-TPO (right) profiles of different catalysts. (a) Ni/SiO₂, (b) Ni/5La₂O₃-SiO₂, (c) Ni/10La₂O₃-SiO₂, (d) Ni/15La₂O₃-SiO₂ and (e) Ni/30La₂O₃-SiO₂.

deactivated slightly. The catalytic activity of Ni catalysts on La₂O₃-modified SiO₂ was remarkably enhanced when the added amount of La₂O₃ is above 10 wt% and the detected conversion of methane remained stable during 5 h.

Table 3
The amount of coke over Ni/SiO₂ and Ni/30La₂O₃-SiO₂ catalysts

Catalyst	Coke (mmol/g-cat)		
	Total coke	Removed by CO ₂	Inactive carbons
Ni/SiO ₂	12.9	10.4	2.5
Ni/30La ₂ O ₃ -SiO ₂	1.9	1.4	0.5

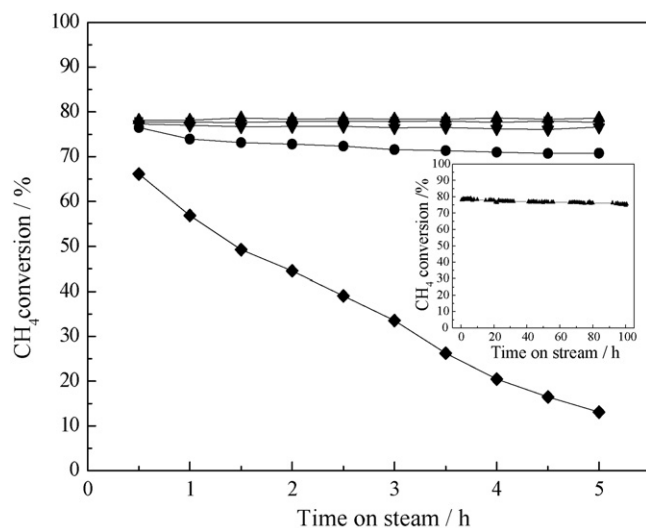


Fig. 7. The effect of La₂O₃ loading on the conversion of CH₄. (◆) Ni/SiO₂, (●) Ni/5La₂O₃-SiO₂, (■) Ni/10La₂O₃-SiO₂, (▼) Ni/15La₂O₃-SiO₂ and (▲) Ni/30La₂O₃-SiO₂.

On Ni/30La₂O₃-SiO₂ catalyst, the conversion of CH₄ reached 78.1% (at 700 °C) in the initial 18 h, and only slightly decreased to 75.5% in the detected 100 h.

4. Conclusion

Ni/*x*La₂O₃-SiO₂ (*x* = 10, 15, 30) catalysts exhibited higher activity and stability for MSTR in fluidized-bed reactor. La₂O₃ strengthened the metal-support interaction and improved the dispersion of Ni. Pulse reactions indicated that CH₄ conversion could be accelerated by CO₂ and O₂, but it increased more rapidly on Ni/30La₂O₃-SiO₂ compared with Ni/SiO₂. The reactivity of surface carbons toward CO₂ and O₂ showed that La₂O₃ reduced the dehydrogenation ability of Ni. O₂ in feed played a crucial role in the gasification of inactive surface carbons, and also in the steadily operation of the autothermal reforming process. These characteristics may be responsible for the higher stability of Ni/*x*La₂O₃-SiO₂ (*x* = 10, 15, 30) catalysts.

Acknowledgments

This project was financially supported by the National Natural Science Foundation of China (Contract no. 20433030), the Ministry of Science and Technology of China through the National Key Project of Fundamental Research (Contract no. 2007CB210207) and State Key Laboratory Breeding Base of Green Chemistry-Synthesis Technology.

References

- [1] A.T. Ashcroft, A.K. Cheetham, M.L.H. Green, P.D.F. Vernon, *Nature* 352 (1991) 225.

- [2] Y.H. Hu, E. Ruckenstein, *Adv. Catal.* 48 (2004) 297.
- [3] Q.S. Jing, H. Lou, J.H. Fei, Z.Y. Hou, X.M. Zheng, *Int. J. Hydrogen Energy* 29 (2004) 1245.
- [4] X. Chen, K. Honda, Z.G. Zhang, *Catal. Today* 93–5 (2004) 87.
- [5] E. Ruckenstein, H.Y. Wang, *Catal. Lett.* 73 (2001) 99.
- [6] A.M. O'Connor, J.R.H. Ross, *Catal. Today* 46 (1998) 203.
- [7] M.M.V.M. Souza, M. Schmal, *Appl. Catal. A: Gen.* 255 (2003) 83.
- [8] V.R. Choudhary, A.M. Rajput, B. Prabhakar, *Catal. Lett.* 32 (1995) 391.
- [9] B.T. Li, S. Kado, Y. Mukainakano, T. Miyazawa, T. Miyao, S. Naito, K. Okumura, K. Kunimori, K. Tomishige, *J. Catal.* 245 (2007) 144.
- [10] K. Tomishige, Y. Matsuo, Y. Yoshinaga, Y. Sekine, M. Asadullah, K. Fujimoto, *Appl. Catal. A: Gen.* 223 (2002) 225.
- [11] E. Ruckenstein, Y.H. Hu, *Ind. Eng. Chem. Res.* 37 (1998) 1744.
- [12] V.R. Choudhary, K.C. Mondal, A.S. Mamman, *J. Catal.* 233 (2005) 36.
- [13] B.T. Li, K. Maruyama, M. Nurunnabi, K. Kunimori, K. Tomishige, *Ind. Eng. Chem. Res.* 44 (2005) 485.
- [14] B.T. Li, K. Maruyama, M. Nurunnabi, K. Kunimori, K. Tomishige, *Appl. Catal. A: Gen.* 275 (2004) 157.
- [15] Y. Matsuo, Y. Yoshinaga, Y. Sekine, K. Tomishige, K. Fujimoto, *Catal. Today* 63 (2000) 439.
- [16] E. Ruckenstein, Y.H. Hu, *J. Catal.* 161 (1996) 55.
- [17] K. Tomishige, *Catal. Today* 89 (2004) 405.
- [18] Q.S. Jing, H. Lou, L.Y. Mo, J.H. Fei, X.M. Zheng, *J. Mol. Catal. A: Chem.* 212 (2004) 211.
- [19] Z.L. Zhang, X.E. Verykios, S.M. MacDonald, S. Affrossman, *J. Phys. Chem.* 100 (1996) 744.
- [20] V.A. Tsipouriari, X.E. Verykios, *Catal. Today* 64 (2001) 83.
- [21] A. Slagtern, Y. Schuurman, C. Leclercq, X. Verykios, C. Mirodatos, *J. Catal.* 172 (1997) 118.
- [22] V.A. Tsipouriari, Z. Zhang, X.E. Verykios, *J. Catal.* 179 (1998) 283.
- [23] Z.L. Zhang, V.A. Tsipouriari, A.M. Efstathiou, X.E. Verykios, *J. Catal.* 158 (1996) 51.
- [24] Z.Y. Hou, O. Yokota, T. Tanaka, T. Yashima, *Catal. Lett.* 89 (2003) 121.
- [25] S. Wang, G.Q. Lu, *Energy Fuel* 12 (1998) 248.
- [26] E.P. Barrett, L.G. Joyner, P.P. Halenda, *J. Am. Chem. Soc.* 73 (1951) 373.
- [27] G. Sewell, C. O'Connor, E. Steen, *Appl. Catal. A: Gen.* 125 (1995) 99.
- [28] F. Pompeo, N.N. Nichio, M.G. Gonzalez, M. Montes, *Catal. Today* 107–108 (2005) 856.
- [29] Z. Xu, Y.M. Li, J.Y. Zhang, L. Chang, R.Q. Zhou, Z.T. Duan, *Appl. Catal. A: Gen.* 210 (2001) 45.
- [30] B.Q. Xu, J.M. Wei, Y.T. Yu, Y. Li, J.L. Li, Q.M. Zhu, *J. Phys. Chem. B* 107 (2003) 5203.
- [31] M.C.J. Bradford, M.A. Vannice, *Catal. Rev.* 41 (1999) 1.
- [32] C.N. Triantafyllopoulos, S.G. Neophytides, *J. Catal.* 239 (2006) 187.
- [33] D.L. Trimm, *Catal. Today* 49 (1999) 3.
- [34] Z.Y. Hou, T. Yashima, *Catal. Lett.* 89 (2003) 193.
- [35] Z.Y. Hou, T. Yashima, *Appl. Catal. A: Gen.* 261 (2004) 205.
- [36] P. Chen, Z.Y. Hou, X.M. Zheng, T. Yashima, *React. Kinet. Catal. Lett.* 85 (2005) 51.
- [37] V.C.H. Kroll, H.M. Swaan, C. Mirodatos, *J. Catal.* 161 (1996) 409.
- [38] V.C.H. Kroll, H.M. Swaan, S. Lacombe, C. Mirodatos, *J. Catal.* 164 (1996) 387.
- [39] S. Wang, G.Q. Lu, *Ind. Eng. Chem. Res.* 38 (1999) 2615.
- [40] J.H. Lee, E.G. Lee, O.S. Joo, K.D. Jung, *Appl. Catal. A: Gen.* 269 (2004) 1.
- [41] A. Santos, M. Menendez, A. Monzon, J. Santamaria, E.E. Miro, E.A. Lombardo, *J. Catal.* 158 (1996) 83.
- [42] G.S. Gallego, F. Mondragon, J. Barrault, J.M. Tatibouet, C. Batiot-Dupeyrat, *Appl. Catal. A: Gen.* 311 (2006) 164.